

INCORPORATION OF A TWO-FLUX MODEL FOR RADIATIVE HEAT TRANSFER IN A COMPREHENSIVE FLUIDIZED BED SIMULATOR. PART II: NUMERICAL RESULTS AND ASSESSMENT

José Antonio Rabi

UNICAMP – State University at Campinas, Faculty of Mechanical Engineering, C. Postal 6122, Campinas, SP, Brazil, 13087-970
jrabi@fem.unicamp.br

Márcio Luiz de Souza-Santos

UNICAMP – State University at Campinas, Faculty of Mechanical Engineering, C. Postal 6122, Campinas, SP, Brazil, 13087-970
jrabi@fem.unicamp.br

***Abstract.** As shown in the first part of this paper, equations and considerations for a preliminary attempt to improve the treatment for radiative heat transfer of a previous comprehensive simulation program were presented. For that, the two-flux radiative heat transfer model was applied. In this second part, the new version of that program was tested against steady-state operations of real equipment. Numerical simulations were carried for two different fluidized-bed reactors: a coal-fed boiler and a wood-fed gasifier. Computational results obtained with that new version were compared with those obtained with the previous simulator version. Then, both sets of results were also compared with real operational data. Special attention was paid to the temperature profiles of each particle species present in the bed section – carbonaceous, limestone and inert – as well as to the radiative heat transfer rates between these solids. Effects on the temperature profiles of the gas phases – emulsion and bubbles – and on the equipment performance parameters were also investigated. Improvements related to the incorporation of two-flux model are assessed and discussed. New developments and extensions of this approach are indicated.*

***Keywords.** numerical simulation, bubbling fluidized bed, thermal radiation, flux method*

1. Introduction

Bubbling fluidized bed equipments have been extensively employed in industrial processes such as combustion and gasification. Over the last two decades, several comprehensive mathematical model and computational program for such equipments has been developed. Among them, the approach started at the University of Sheffield (de Souza-Santos, 1987, 1989) has been continuously improved (de Souza Santos, 1989, 1992, 1993, 1994a,b, 1996, 1997, 1998 and 1999). Currently, the simulator counts up to 100-coupled differential equations describing the mass and energy balances. In addition, equations and relationships related to chemical reaction kinetics, fluidization dynamics, entrainment and attrition of particles, as well as several other processes compose that simulator. Despite its success, the simulator has employed a simple approach for thermal radiation exchanges. In cases of relatively high temperatures, thermal radiation becomes a very important heat transfer mode. Therefore, too simple models might lead to deviations above acceptable levels. Aiming to improve the treatment used in the current version of the simulator, the present work has introduced a two-flux model for the radiative heat transfer between all solid species present in the emulsion.

The first part of this paper (Rabi and de Souza-Santos, 2002) describes a two-flux approximation under a non-homogeneous polydispersed particulate media in radiative equilibrium approach. The newly developed model equations are again presented for quick reference. Definitions of all quantities may be found in the above-mentioned paper.

2. Summary of the newly introduced model equations

At a given bed height z , the former radiative heat transfer rate $E_{R,SESE,m}$ ($\text{W}\cdot\text{m}^{-1}$) referring to a m -type particles ($m = 1$ for carbonaceous, $m = 2$ for limestone and $m = 3$ for inert) in the emulsion has been replaced to

$$E_{R,SESE,m} = S_E K_{a,m} (4\sigma T_{SE,m}^4 - G) \quad (1)$$

where S_E is the emulsion sectional area (m^2 , including interstitial gas), σ is the Stefan-Boltzmann constant and $T_{SE,m}$ is the particle local temperature (K). In a two-flux model, the incident radiation function G ($\text{W}\cdot\text{m}^{-2}$) is evaluated in terms of the forward and backward radiation intensities according to

$$G(z) = 2\pi[I^+(z) + I^-(z)] \quad (2)$$

The absorption coefficient $K_{a,m}$ (m^{-1}) corresponding to a polydispersed particulate medium is given by

$$K_{a,m} = \frac{1.5f_m'''(1-\nu_E)\varepsilon_{S,m}}{\bar{d}_{S,m}} \quad (3)$$

Here, f_m''' is the solid volume fraction, $\varepsilon_{S,m}$ is its emissivity, $\bar{d}_{S,m}$ is its mean diameter and ν_E is the emulsion void fraction. The scattering counterpart is given by

$$K_{s,m} = \frac{1.5f_m'''(1-\nu_E)(1-\varepsilon_{S,m})}{\bar{d}_{S,m}} \quad (4)$$

Moreover, independent absorption and scattering was evoked so that bulk absorption and scattering coefficients K_a and K_s are obtained by summing up optical characteristics from each solid species as

$$K_a = \sum_m K_{a,m} \quad \text{and} \quad K_s = \sum_m K_{s,m} \quad (5)$$

It was shown that radiative equilibrium condition prevailed inside the particulate medium. As a consequence, $I^+(z)$ and $I^-(z)$ are no longer independent but related to each other according to

$$I^+(z) + I^-(z) = \frac{2\sigma}{\pi} \frac{1}{K_a} \sum_m K_{a,m} T_{SE,m}^4 \quad (6)$$

It is always important to mention that the above condition holds only for a two-flux approximation. Therefore, only one transfer equation needs to be solved, namely, for the forward radiation intensity,

$$\frac{1}{2} \frac{dI^+}{dz} = -(K_a + K_s)I^+ + \sum_m K_{a,m} \frac{\sigma T_{SE,m}^4}{\pi} + \frac{K_s}{4\pi} G(z) \quad (7)$$

subjected to the following boundary condition

$$I^+(0) = \frac{\sigma}{\pi} \left[\frac{2(1-\varepsilon_d)}{2-\varepsilon_d} \frac{1}{K_a} \sum_m K_{a,m} T_{SE,m}^4(0) + \frac{\varepsilon_d}{2-\varepsilon_d} T_d^4 \right] \quad (8)$$

which depends upon the distributor plate emissivity ε_d and temperature T_d as well as on the particle temperatures at the bed base ($z = 0$). The temperature T_d is calculated by iterative process based upon an empirical correlation (Zhang and Ouyang, 1985) used since the early versions of the program (de Souza-Santos, 1987).

The energy balance for a m -type solid in the emulsion (bed section) is then expressed by

$$F_{SE,m} c_{S,m} \frac{dT_{SE,m}}{dz} = -E_{Q,SE,m} - E_{M,SEGE,m} - E_{C,SEGE,m} - \sum_{n=1}^3 E_{C,SESE,m,n} - E_{R,SESE,m} - E_{R,SETD,m} - E_{R,SEWD,m} \quad (9)$$

where $F_{SE,m}$ is the solid mass flow ($kg \cdot s^{-1}$) and $c_{S,m}$ its specific heat ($J \cdot kg^{-1} \cdot K^{-1}$). The meaning of each energy source or sink term ($W \cdot m^{-1}$) on the right hand side of the above equation was explained in the first part of the paper.

3. Basic description of the simulation computational program

The computational program was written in Fortran language and corresponds to the numerical implementation of the mathematical model. Therefore, it simulates steady-state operations of axially symmetric bubbling fluidized bed equipments so that all physical quantities and operational parameters depend only on the bed height z . In order to accomplish this task, the program is divided into several modules and routines.

As far as energy balances are concerned in the bed and freeboard sections, the simulator takes into account several heat transfer modes involving different phases in the emulsion (gas and solid species), bubbles, immersed tubes, reactor walls and distributor plate. The present work is particularly interested in heat transfers through thermal radiation between all solid species in the emulsion (bed section). These are related to the term $E_{R,SESE,m}$ in the energy balance equation, Eq. (9). As a simplification, both emulsion interstitial gas and gas in the bubbles are assumed transparent to thermal radiation. Therefore, there are no terms corresponding to radiative heat transfers involving any gas phase.

Although a quite similar approach can be followed for the freeboard section, the corresponding radiative heat transfer equations for that section are not presented in this preliminary work. This is left for a near future publication.

Heat transfer between the external reactor wall and the environment and between the internal wall of tubes and steam or liquid water inside them are considered as well. Figure (1) below shows a schematic representation of heat and mass transfers adopted and implemented in the program (de Souza-Santos, 1987).

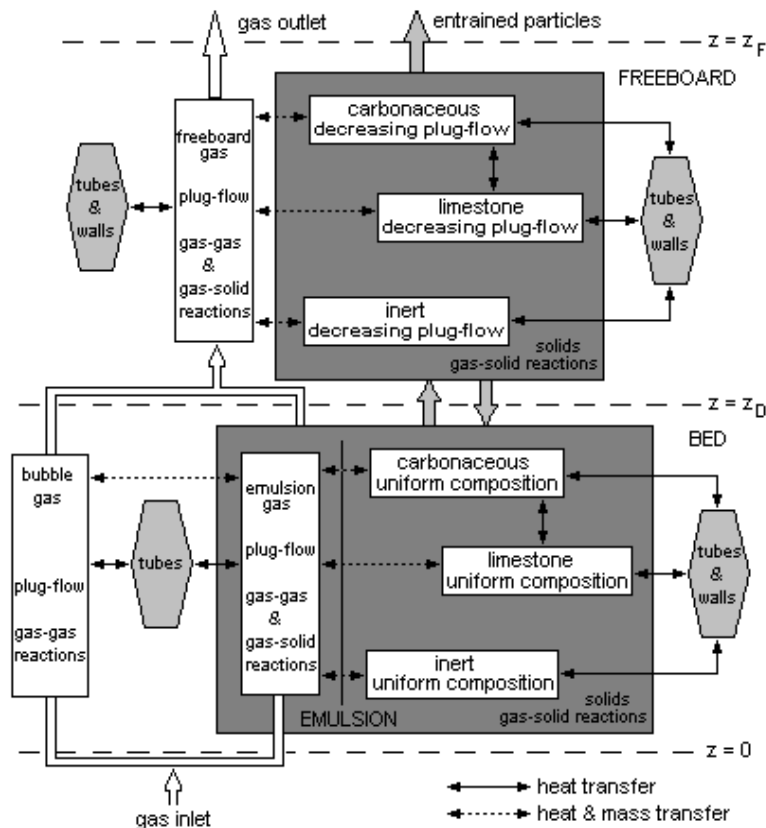


Figure 1. Schematic representation of heat and mass transfers implemented in the computational program.

The basic necessary input data for the simulation program comprise:

- Physical and chemical characterization of the fed carbonaceous, limestone and inert solids;
- Characterization of the gaseous agent injected through the distributor;
- Complete description of the equipment geometry.

On the other hand, the basic characteristics and results that can be provided by the program include:

- Concentration profiles of 20 gaseous components (H_2 , H_2O , CO , CO_2 , O_2 , N_2 , CH_4 , SO_2 , NO , NO_2 , N_2O , H_2S , NH_3 , C_2H_4 , C_2H_6 , C_3H_6 , C_3H_8 , C_6H_6 , Tar) throughout the bed (emulsion and bubbles) and the freeboard;
- Flow and temperature profiles of gases in the bed and freeboard.
- Temperature, rate of circulation profiles (or flow) of solid phase components in the bed and freeboard;
- Composition, particle size distribution of each solid species in the bed and at each point of the freeboard;
- At each point of the equipment, all important parameters related to the bed and freeboard dynamics, among them: bubble diameters, upward velocities of each phase (emulsion, bubbles, particles), minimum fluidization parameters, rate of particle turnovers, etc.;
- In cases of recycling of solid collected by the cyclones, all parameters describing such operation and its effects in the process;
- Profiles of individual rates of all homogeneous and heterogeneous reactions (around 30 in each phase: emulsion, bubble, freeboard). This can provide a clear picture for deeper understanding of the processes occurring at each point of the equipment;
- Important engineering parameters to help in design as well as optimization of equipment and operations.

4. Numerical results and assessment

The previously reported thermal radiation equations account for a small portion of the whole set of equations in the comprehensive mathematical model for fluidized bed processes. Nevertheless, the incorporation of the two-flux model could in principle improve the quality of the numerical results. This issue is now assessed through comparisons between simulations and real operation data.

Two different fluidized bed reactors were chosen in order to carry out numerical simulations: a coal-fed combustor boiler and a wood-fed gasifier. Computational results from the modified version (“new” radiative heat transfer model) are compared with results from the previous version (“old” radiative heat transfer model). These are also compared against data obtained from real fluidized bed operations.

4.1. Simulation of a coal-fed combustor boiler

Some basic data regarding plant operation and the equipment are shown in Tab. (1). It corresponds to a Babcock & Wilcox (1976) boiler pilot unit.

Table 1. Basic data for the Babcock & Wilcox unit and operational conditions for the test number 26.

Characteristic	Value
Coal proximate analysis (wet basis - % mass)	
Moisture	5.0
Volatiles	38.0
Fixed carbon	47.6
Ash	9.4
Coal ultimate analysis (dry basis - % mass)	
C	73.2
H	5.1
O	7.9
N	0.9
S	3.0
Ash	9.9
Inlet gas through distributor (wet basis - % mass)	
N ₂	75.428
O ₂	22.785
H ₂ O	1.201
CH ₄	0.432
C ₂ H ₆	0.154
Boiler basic geometry	
Equivalent diameter: $D_D = D_F$ (m)	1.118
Bed height: z_D (m)	0.700
Freeboard height: z_F (m)	3.442
Feeding point height: z_{FEED} (m)	0.305
Tube bank	
Number of tubes in the freeboard	30
Length of each tube (m)	0.991
Bottom bed tube position: z_{TUDB} (m)	0.330
Top bed tube position: z_{TUDT} (m)	0.700
External diameter (m)	0.0483
Internal diameter (m)	0.0409
Flow of coal (kg.s ⁻¹)	0.0585
Flow of limestone (kg.s ⁻¹)	0.01215

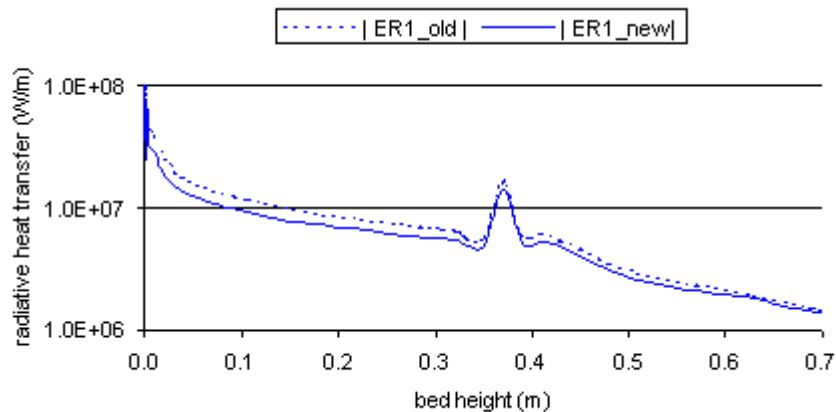


Figure 2. Radiative heat transfer profiles in the bed section (absolute values) for carbonaceous solid.

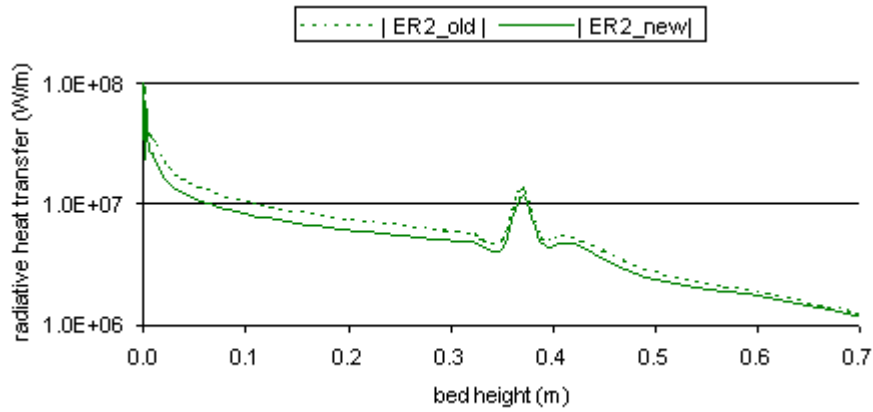


Figure 3. Radiative heat transfer profiles in the bed section (absolute values) for limestone.

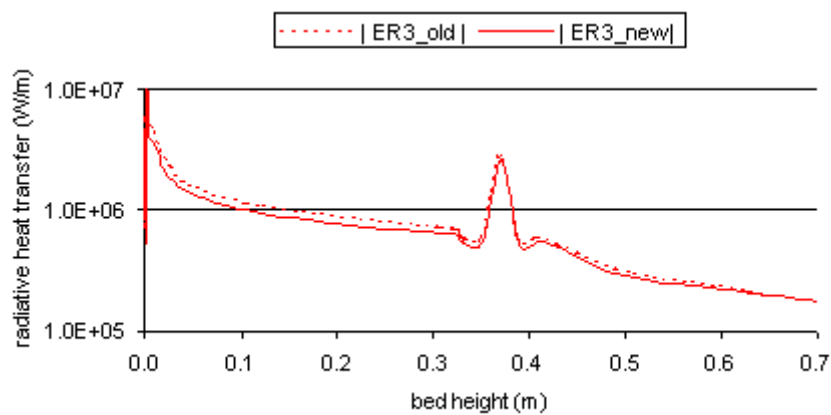


Figure 4. Radiative heat transfer profiles in the bed section (absolute values) for inert solid.

Figures (2), (3) and (4) shows the radiative heat transfer profiles along the bed axial coordinate z for carbonaceous solid $E_{RSESE,1}$, for limestone $E_{RSESE,2}$ and for inert solid $E_{RSESE,3}$, respectively. Although results showed that $E_{RSESE,1}$ was always strictly positive, absolute values were plotted because $E_{RSESE,2}$ and $E_{RSESE,3}$ were negative, thus preventing a logarithmic graph. The numerical results from the two-flux (new) approach were slightly lower in absolute values than those from the original (old) model. However, despite of these differences, all profiles followed a similar trend.

The temperature profiles along the bed section for carbonaceous solid, for limestone and for inert solid are shown respectively in Figs. (5), (6) and (7), whereas Fig. (8) shows the temperature profiles for both emulsion (interstitial) and bubble gas. Although the new radiative heat transfer model does not affect directly the energy balance equations for the gaseous phases (as gas was assumed transparent to thermal radiation), differences in the temperature profiles of solids influenced the thermal behavior of the emulsion gas (in greater extent due to its close contact to solids) and of the bubble gas. Of course, that was expected. Nevertheless, new predicted values are slightly higher for all phases and all profiles followed a similar trend.

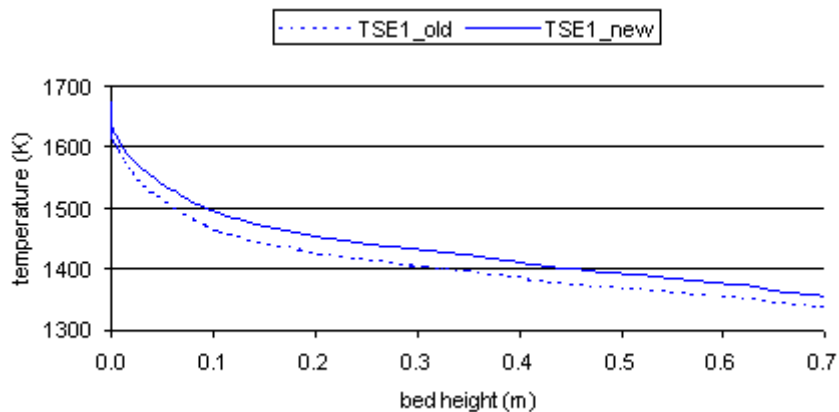


Figure 5. Temperature profiles for carbonaceous solid in the bed section.

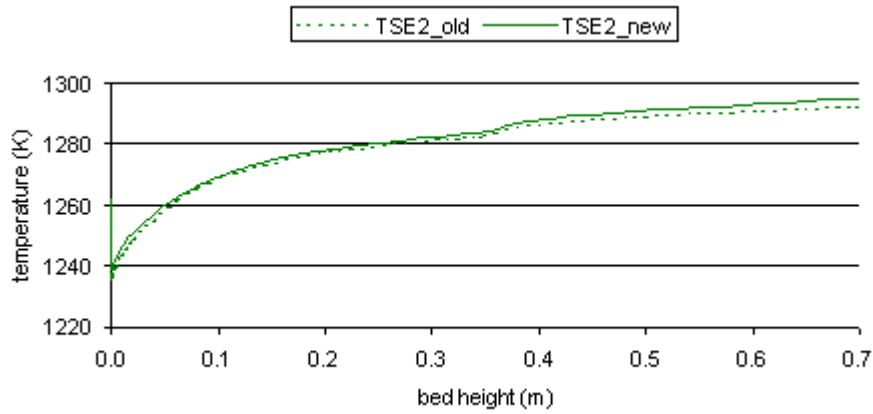


Figure 6. Temperature profiles for limestone in the bed section.

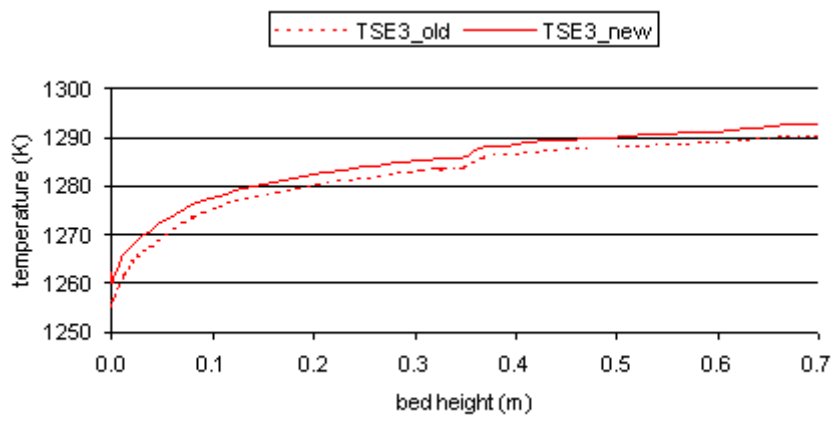


Figure 7. Temperature profiles for inert solid in the bed section.

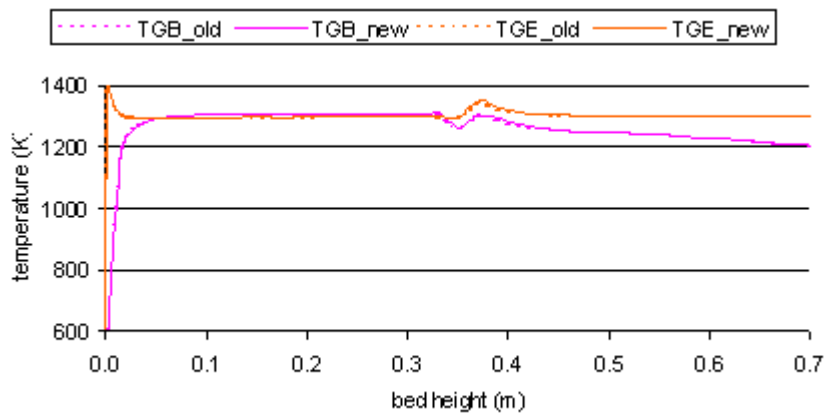


Figure 8. Temperature profiles for emulsion (interstitial) and bubble gas in the bed section.

Table 2. Available composition (molar %, dry basis) of the gas leaving the freeboard (stack gas).

Components	Experimental	Simulation – old	Simulation – new
CO ₂	13.8	15.42	15.34
CO	0.0 to 0.9	0.03	0.00
O ₂	3.9	2.91	3.01
N ₂	81.2	81.53	81.54
NO	0.03	0.03	0.03
SO ₂	0.08	0.08	0.08

Tables (2) and (3) allow comparisons between simulated results (from the old and from the new mathematical model) against real operational parameters. These later data refer to a real operation of a boiler pilot unit (Babcock & Wilcox, 1976). From these tables, it can be verified that the two-flux approach did not yield significant improvements.

Table 3. Some process parameters for operation of the Babcock & Wilcox pilot unit, test no. 26.

Parameter	Experimental	Simulation – old	Simulation – new
Mass flow of flue gas (kg.s^{-1})	0.790	0.748	0.748
Superficial velocity at the middle of the bed (m.s^{-1})	2.5	2.6	2.6
Carbon conversion (fraction of fed carbon, %)	95.8	93.98	93.05
Calcium conversion (%)	28.09	25.28	25.16
Sulphur retention (based on fed sulphur, %)	58.7	57.83	57.54
Calcium to sulphur (Ca/S) ration in bed	2.2	2.29	2.29
Total heat transfer to tubes in the system (kW)	788.4	776.0	786.0
Temperature of water leaving tubes (K)	400	463.7	463.7

4.2. Simulation of a wood-fed gasifier

Some basic data regarding plant operation and the equipment are shown in Tab. (4). It corresponds to pressurized fluidized-bed gasifier for wood – RENUGAS pilot unit (Evans et al., 1986). Note that in this case no limestone is fed.

Table 4. Basic data for the operational conditions for RENUGAS pilot unit.

Characteristic	Value
Wood proximate analysis (wet basis - % mass)	
Moisture	4.94
Volatiles	79.39
Fixed carbon	14.90
Ash	0.77
Wood ultimate analysis (dry basis - % mass)	
C	48.40
H	6.31
O	44.23
N	0.21
S	0.03
Ash	0.82
Inlet gas and solid feedings	
Mass flow of wood at $z = 0.381$ (kg.s^{-1})	0.08113
Mass flow of O_2 through the distributor (kg.s^{-1})	0.020575
Mass flow of steam through the distributor (kg.s^{-1})	0.049215
Mass flow of N_2 at $z = 0.381$ (kg.s^{-1})	0.043772
Inlet temperature of O_2 (K)	644
Inlet temperature of steam (K)	672
Inlet temperature of N_2 (K)	293
Gasifier basic geometry	
Bed equivalent diameter: D_D (m)	0.292
Bed height: z_D (m)	1.585
Freeboard equivalent diameter: D_F (m)	0.451
Freeboard height: z_F (m)	6.147
Feeding point height: z_{FEED} (m)	0.381

The radiative heat transfer profiles along the bed section for carbonaceous solid are shown in Fig. (9). Absolute values were also considered because this term is initially positive (heat loss) until approximately $z = 0.35$ m, where it became negative for the first time. It swapped signs a few more times further along the bed. In this case, the two profiles (from the new and from the old model) followed a similar trend reasonably well up to the middle of the bed.

As no limestone ($m = 2$) was considered in the gasification process, identical graphs (not shown for simplicity) as those in Fig. 9 were obtained for the radiative heat transfer profiles regarding the inert solid. This is in accordance to the radiative equilibrium condition, namely $\sum E_{\text{RSESE},m} = 0$, discussed in the first part of this paper. In other words, $E_{\text{RSESE},3}$ assumed the very same absolute values as $E_{\text{RSESE},1}$ did, but having opposite sign.

There were only small differences between the temperature profiles for the two solid species present in the bed, as seen in Figs. (10) and (11). New predicted values are slightly higher for both of them. Practically no differences can be observed for the emulsion (interstitial) gas and bubble gas temperature profiles, as shown in Fig. (12). It is interesting to note that the temperature drop due to the intermediate cold gas (N_2) injection at $z = 0.381$ m was neatly reproduced by both radiative heat transfer approaches.

Subsequently, Tabs. (5) and (6) compare some simulated results (old and new approaches) against experimental data. These later values correspond to a real operation of a gasifier pilot unit (Evans et al., 1986), namely RENGAS from IGT – Institute of Gas Technology (Chicago, USA). Once again, it can be verified that the two-flux approach for radiative heat transfer did not yield significant improvements.

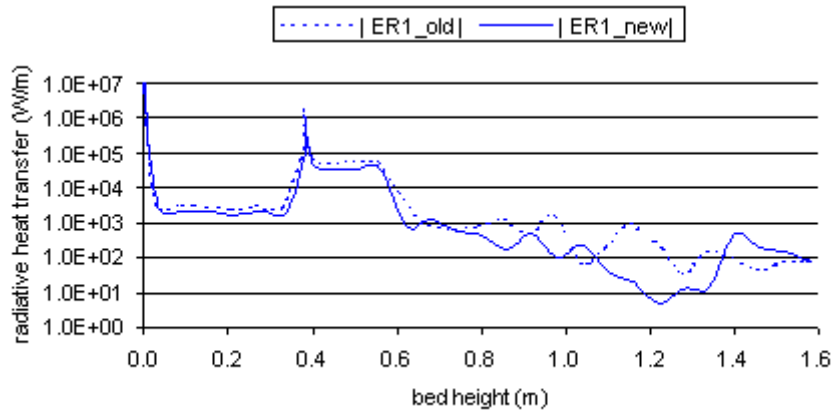


Figure 9. Radiative heat transfer profiles in the bed section (absolute values) for carbonaceous solid.

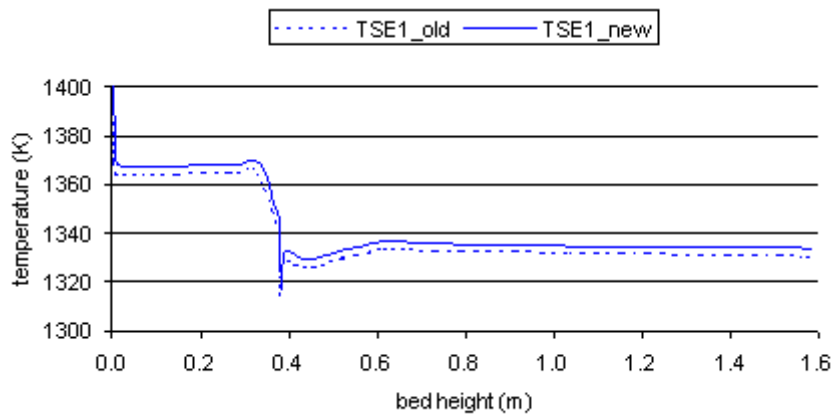


Figure 10. Temperature profiles for carbonaceous solid in the bed section.

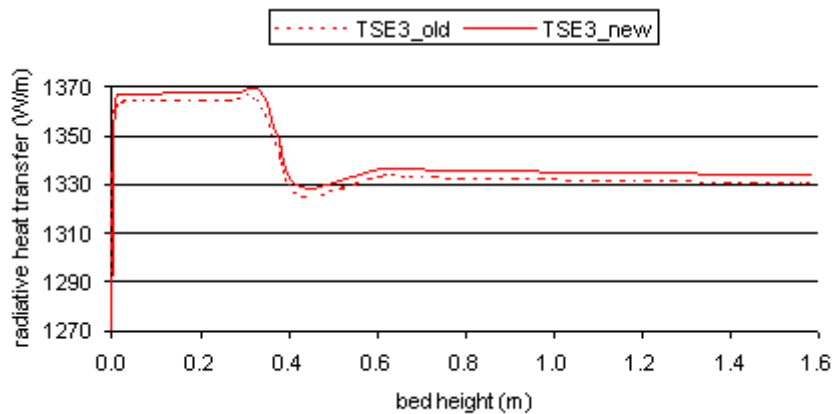


Figure 11. Temperature profiles for inert solid in the bed section.

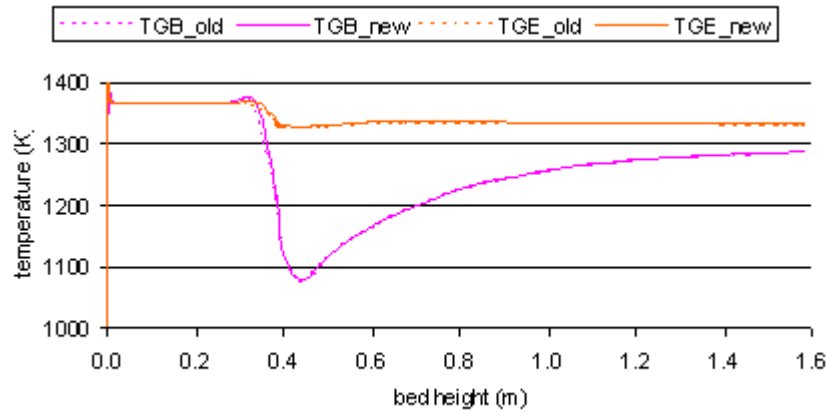


Figure 12. Temperature profiles for emulsion (interstitial) and bubble gas in the bed section.

Table 5. Available composition (volume %, wet basis) of the produced gas.

Components	Experimental	Simulation - old	Simulation – new
CO ₂	17.06	15.75	15.60
CO	8.00	10.63	10.26
H ₂ O	35.82	34.24	34.64
H ₂	12.05	13.37	13.08
N ₂	19.18	18.49	18.77
CH ₄	7.37	6.93	7.04
C ₂ H ₄	0.03	0.03	0.03
C ₂ H ₆	0.22	0.22	0.23
C ₃ H ₈	0.00	0.00	0.00
C ₆ H ₆	0.27	0.28	0.29

Table 6. Some conditions and parameters for gasification process.

Condition or parameter	Experimental	Simulat. - old	Simulat. - new
Total mass flow of produced gas	0.1843 kg/s	0.1943 kg/s	0.1914 kg/s
Mass flow of solid entrained at the top of the freeboard	0.210E-4 kg/s	0.168E-3 kg/s	0.162E-3 kg/s
Superficial gas velocity at the middle of the bed	0.52 m/s	0.26 m/s	0.26 m/s
Average temperature at the middle of the bed	1105 K	1315 K	1318 K
Carbon conversion to gas	90.2%	96.75%	94.31%
Combustion enthalpy of the produced gas (dry, clean, at 298 K)	7.31 MJ/kg	7.80 MJ/kg	7.79 MJ/kg

5. Concluding remarks

Following a two-flux approach for a non-homogeneous participating media in radiative equilibrium, an attempt has been made to improve the simulation of the radiative heat transfer between all solid particles in fluidized bed equipment like gasifiers and boilers. The resulting equations were incorporated into the energy balance equations proposed for the bed section by an existing comprehensive mathematical model and simulation program.

Comparisons between simulated results from the new approach and from the previous version against operational conditions of real bubbling fluidized-bed boiler and gasifier units showed almost no significant differences. This picture might change if the new model is to be extended for the freeboard section, where particles are further apart and tubes for steam generation are immersed. In this case, the assumption of transparent gases between particles becomes more critical. That issue of the two-flux model incorporation claims for further assessment.

6. Acknowledgement

The authors are grateful to FAPESP – Fundação de Amparo à Pesquisa do Estado de São Paulo, for their financial support to the research project (process no. 98/02891-8).

7. References

- Babcock & Wilcox, 1976, EPRI FP-308, vol. 2.
- de Souza-Santos, M.L., 1987, "Modeling and Simulation of Fluidized-Bed Boilers and Gasifiers for Carbonaceous Solids", Ph.D. Thesis, University of Sheffield, Department of Chemical Engineering and Fuel Technology, England.
- de Souza-Santos, M.L., 1989, "Comprehensive Modeling and Simulation of Fluidized-Bed Boilers and Gasifiers", *Fuel*, Vol. 68, pp. 1507-1521.
- de Souza-Santos, M.L., 1992, "Application of Comprehensive Simulation to Pressurized Fluidized-Bed Hydroretorting of Shale", Eastern Oil Shale Symposium, Lexington, Kentucky, USA.
- de Souza-Santos, M.L., 1993, "Comprehensive Modeling and Simulation of Fluidized-Bed Reactors Used in Energy Generation Processes, Meeting on Energy Modeling Optimizing Information and Resources, IGT – Institute of Gas Technology, Chicago, USA.
- de Souza-Santos, M.L., 1994a, "Application of Comprehensive Simulation to Pressurized Fluidized-Bed Hydroretorting of Shale", *Fuel*, Vol. 73, No. 9, pp. 1459-1465.
- de Souza-Santos, M.L., 1994b, "Application of Comprehensive Simulation of Fluidized-Bed Reactors to the Pressurized Gasification of Biomass", *J. of the Braz. Soc. Mechanical Sciences*, Vol. XVI, No. 4, pp. 376-383.
- de Souza-Santos, M.L., 1996, "Otimização Teórica e Testes Experimentais Preliminares de Gaseificação de RASF em Leito Fluidizado", IPT – Instituto de Pesquisas Tecnológicas do Estado de São Paulo, Report no. 34.926/DME/AET.
- de Souza-Santos, M.L., 1997, "A Study on Pressurized Fluidized-Bed Gasification of Biomass through the Use of Comprehensive Simulation", *Proceedings of the 4th International Conference on Technologies and Combustion for a Clean Environment*, Lisboa, Portugal, Vol. 2, section 25.2, pp. 7-13.
- de Souza-Santos, M.L., 1998, "A Study on Pressurized Fluidized-Bed Gasification of Biomass through the Use of Comprehensive Simulation", In: "Combustion Technologies for a Clean Environment", chapter 4, Gordon and Breach Publishers, Amsterdam, Holland.
- de Souza-Santos, M.L., 1999, "A Feasibility Study on an Alternative Power Generation System Based on Biomass Gasification/Gas Turbine Concept", *Fuel*, Vol. 78, pp. 529-538.
- Evans, R.J, Knight, R.A., Onischak, M., Babu, S.P., 1986. "Process and Environmental Assessment of the RENUGAS Process", *Symposium on Energy from Biomass and Wastes*, IGT – Institute of Gas Technology, Chicago, USA.
- Rabi, J.A., de Souza-Santos, M.L., 2002, "Incorporation of a Two-Flux Model for Radiative Heat Transfer in a Comprehensive Fluidized Bed Simulator. Part I: Preliminary Theoretical Investigations", Submitted to ENCIT 2002, Caxambu, MG, Brazil, Paper CIT02-0712.
- Zhang, G.T., Ouyang, F., 1985, Heat transfer between the fluidized bed and the distributor plate, *Ind. Eng. Chem. Process Des. Dev.*, Vol. 24, pp. 430-433.